Transient Particle Acceleration Associated with Solar Flares

E. L. CHUPP

Understanding how individual charged particles can be accelerated to extreme energies (10^{20} electron volts), remains a foremost problem in astrophysics. Within our solar system, the active sun is capable of producing, on a short time scale, ions with energies higher than 25 gigaelectron volts. Satellite and ground-based observations over the past 30 years have greatly increased our knowledge of the properties of transient bursts of energetic particles emitted from the sun in association with solar flares, but a real understanding of the solar flare particle acceleration process requires greatly refined experimental data. On the practical side, it is also imperative that this problem be solved if man is to venture, for long periods of time, beyond the protective umbrella of Earth's magnetic field, which excludes much of the biologically damaging solar energetic particles. It is only through an understanding of the basic acceleration problem that we can expect to be able to predict the occurrence of a solar flare with lethal solar radiations. For our knowledge of these effects to advance, a new space mission dedicated to studying the high-energy aspects of solar flares at high spatial and energy resolution will be required.

HOW DO INDIVIDUAL CHARGED PARTICLES, ELECTRONS or ions, attain extreme kinetic energies that can be as high as 10^{20} eV for the primary cosmic rays; above 10^{12} eV (1 TeV) for transient phenomena on neutron stars and powerful x-ray sources, such as Cygnus X-3 and Hercules X-1; and above 10^8 eV for the enigmatic γ-ray bursts? Throughout the solar system, particle acceleration is ubiquitous (*1*). The sun occasionally produces transient bursts of relativistic charged particles, which initiate a strong short-term enhancement of the count rate in ground-level monitors of cosmic radiation—the ground-level event (GLE). The most recent example of this occurred on 29 September 1989 when the ground-level monitors and underground monitors (*2*), over the whole Earth, responded dramatically to particles accelerated in a solar flare which occurred on the backside of the visible disk of the sun! Charged particles with energies up to about 25 GeV were produced in this event and reached the Earth along interplanetary magnetic field lines. More frequently, in phase with the sunspot cycle, solar flares produce charged particles with energies typically as high as 100 MeV. A major goal of current research in solar astrophysics is to determine which mechanisms apply to the solar flare case and to test their applicability to other astrophysical sites where transient x-ray and γ-ray bursts occur.

First, it is of interest to recall the beliefs everyone held about solar flare particle acceleration before extensive observations were available from the United States Solar Maximum Mission (SMM) and the Japanese Hinotori satellites. Based primarily on the early (late 1950s and 1960s) observations of Type III, Type II, and Type IV meter-wave radio observations of solar flares and early satellite observations of solar flare x-ray bursts, it was believed that flare-associated particle acceleration occurred in two stages or phases (*3*). In the first stage electrons were accelerated to energies of ~100 keV, giving rise to the Type III radio bursts, a bremsstrahlung x-ray burst and minutes later (typically 10 minutes), in some flares, ions would be accelerated to hundreds of MeV (or GeV) energies by a shock wave, moving outward through the corona and causing the Type II and Type IV radio bursts. This picture gives a straightforward, logical explanation for the high-energy emissions from a solar flare which include the prompt hard x-ray burst at the flare initiation, followed by the delayed production of the accelerated ions which occasionally produce the GLE.

With the discovery of nuclear γ-ray lines (*4*) from two flares during the major August 1972 solar activity, which was a signal of ion acceleration, there was no reason to doubt this scenario since the observations could not put a tight restriction on the time of production of the γ-rays. The γ-ray spectra observed in these events were made with an instrument, on the OSO-7 satellite, which had a time resolution of 3 minutes, and it was not possible to discern shorter γ-ray time structure.

It is now clear that this simple picture is not valid because observations made by the γ-ray spectrometer (GRS) on SMM have shown that both ion and electron acceleration can occur on the time scale of seconds (*5*), and this fact has been confirmed by similar measurements made from the Hinotori satellite (*6*). Further, the expected close correlation of the occurrence of bursts of the solar energetic particles (SEPs) observed in space and γ-ray bursts associated with solar flares has not been observed (*7*). A real understanding of the way in which the sun can accelerate particles is still elusive; however, solution to this problem is essential since it may well apply to other astrophysical phenomena.

Diagnostic Tools

Two different approaches are used to determine the characteristics of the charged particles accelerated in association with solar flares:

1) The most direct and oldest technique is to measure the energy spectra and composition of charged particles (SEPs) observed in space and believed to be associated with a specific solar flare. These

The author is professor of physics and is head of the Gamma-Ray Astronomy Group in the Institute for the Study of Earth Oceans and Space, University of New Hampshire, Durham, NH 03824.

charged particles are transported to the observer from the acceleration region along interplanetary field lines, a process which is complex and little understood for specific events. Corrections must therefore be applied to determine spectra and composition of the initially accelerated solar flare charged particles.

2) More recently, by means of satellites (and balloons), it has been possible to record the secondary neutral radiations produced in the solar atmosphere by the particles accelerated (or energized) in association with the solar flare. These secondary radiations include the electromagnetic emissions in the visible, ultraviolet, soft x-ray, hard x-ray, and γ-ray spectral regions and also high-energy neutrons. These neutral radiations directly reflect the properties of the accelerated particles which interact at the Sun.

Gamma-ray line and continuum emissions (<10 MeV). Theoretical studies (*8*), inspired by the seminal paper of Morrison in 1958 (*9*), give a detailed description of the components of a γ-ray spectrum expected from accelerated solar flare ions interacting with the solar atmosphere. In general, one would expect a plethora of γ-ray lines from de-excitation of excited nuclear levels of the most abundant nuclides in the solar atmosphere. To produce these γ-ray lines, which have energies typically below ~8 MeV, requires that protons of energies ≲50 MeV bombard the solar atmosphere. Other nuclear reactions produce neutrons of energies of a few to tens of MeV, and neutron-deficient radioactive positron emitters. Neutrons emitted in the direction of the photosphere slow down to thermal energies, by elastic scattering on hydrogen nuclei, and can be captured to give the deuteron formation line at 2.223 MeV with a width of ~100 eV, characteristic of photospheric temperatures (~6000 K). The positrons, trapped in sunspot magnetic fields, can eventually annihilate with free electrons or bound electrons giving a distinct line at 0.511 MeV with a width (full width at half maximum) of $\Delta E \simeq 1.1(T_4)^{1/2}$ (kiloelectron volts); where T_4 is the temperature of the annihilation region in units of 10^4 K. Since the lifetimes of the excited nuclear levels are typically very short, $\lesssim 10^{-11}$ s, the time variations of this "prompt" de-excitation spectrum reflects, directly, the time history of the accelerated ions interacting with the constituents of the solar atmosphere. The γ-ray lines resulting from neutron capture and positron annihilation, on the other hand, are "delayed emissions," since the characteristic capture time for the neutrons is ~100 s and positron emitters have half-lives of a few to several minutes. Gamma-ray line emission is usually accompanied by a continuous spectrum of photons resulting from the bremsstrahlung of primary electrons also accelerated in the solar flare (*10*). [If the spectrum of accelerated ions extends above 300 MeV and is sufficiently intense, then pion production can lead to an additional contribution to the continuous γ-ray spectrum at higher energies (>10 MeV).]

The first observed γ-ray line spectra from solar flares showed strong lines from neutron capture and positron annihilation at 2.223 MeV and 0.511 MeV, respectively. Weaker nuclear de-excitation lines at 4.438 MeV and 6.129 MeV, from ^{12}C and ^{16}O, respectively, were also identified (*4*). The neutron capture line was later observed during intense flares in 1978 and 1979 (*11*). During the lifetime of the SMM satellite 14 February 1980 to 2 December 1989, with a scaled-up version (*12*) of the OSO-7 γ-ray spectrometer, ~250 additional solar flare γ-ray spectra were obtained with emissions above 300 keV. Figure 1 shows the time-integrated count spectrum (*13*) obtained during an intense, long-duration (~30 min) limb flare on 27 April 1981. This experimental spectrum consists of several nuclear de-excitation lines, from the nuclides indicated, and delayed lines at 0.511 MeV and 2.223 MeV, a continuum consisting of kinematically broadened de-excitation lines and a primary electron bremsstrahlung spectrum extending above 1 MeV. The spectrum runs from ~400 keV to the nuclear ledge at ~7 MeV. This rich nuclear line spectrum can be used to obtain model-dependent solar abundances by matching predicted spectra with the observed spectrum with the use of the instrument response function.

This procedure may be illustrated by considering the instantaneous production rate of an excited nuclide, in thin target geometry expressed as

$$q_{ij} = \int_0^\infty N_i(E,t) n_j c\beta_i(E) \sigma_{ij}(E) dE \quad (1)$$

where i, j refer to the accelerated ion and target nuclide, respectively. $N_i(E,t)$ is the instantaneous number density of particles i with a kinetic energy per nucleon in the range E to $E + dE$, n_j is the number density of the target nuclides, $c\beta_i(E)$ is the velocity of ion i, and $\sigma_{ij}(E)$ is the inelastic cross section for production of a nuclide in an excited state for which γ-ray emission is allowed (in general, this includes spallation reactions). For prompt nuclear de-excitation, the production rate gives the emission rate of photons, so a measurement of the intensity of a given γ-ray line and a theoretical model for the accelerated ion spectrum permits a determination of the density (or abundance) of the target nuclide (*14*). The angular relationship of the bombarding ions with respect to the target and observer must also be considered since the kinematics of the particular reaction can lead to observable broadening or a centroid shift of the de-excitation line. For isotropic reaction geometries the lines are broadened about their rest energy. Also some excited nuclides may have significant recoil velocities ($\gtrsim 10^{-3}\ c$), and the lines will be greatly broadened or their centroid shifted.

Similar model calculations have been carried out for the ion spectrum impinging on a thick target, where all recoiling nuclides and the incident ions stop. In the solar case a so-called "narrow line" spectrum results from protons and α particles incident on the ambient "thick" target of heavier nuclides. Since the accelerated beam of ions is also assumed to contain heavier nuclides, they become excited when impinging on the ambient (predominately hydrogen and helium) target, and their de-excitation lines are greatly broadened, effectively producing a continuum below the narrow lines (*15*).

To determine solar target abundances from the experimental spectrum shown in Fig. 1, an unnormalized de-excitation γ-ray spectrum is calculated for a particular accelerated particle energy spectrum with different assumed compositions for the ions and also an assumed composition for the target abundances (*14*). To this spectrum the delayed γ-rays at 0.511 MeV and 2.223 MeV must be added. For comparison with the experimental observations a continuum due to a primary (power-law) electron bremsstrahlung spectrum is also added to the line spectrum. This introduces additional other parameters, the power-law index and the intensity. This composite spectrum with the several unknown parameters is then folded through the SMM GRS spectrometer response function and a best fit to the experimental spectrum is found by varying the several individual parameters until the overall χ^2 is minimized. Murphy *et al.* (*14*) used this technique, and assuming that the accelerated particle composition was similar to the SEP flux observed in large flares, they found that the best fit was obtained by enhancing the target abundances for Mg, Si, and Fe (relative to C) over the photospheric or local galactic abundances with the results consistent with coronal abundances. Also they noted that the Ne/C ratio was larger than the coronal value, but the O/C ratio (*16*) was, within error, in agreement with both the best photospheric and coronal values. The enhancement of heavier elements ($Z > 8$), is consistent with earlier calculations (*17*).

A further analysis of these data (*18*) varied the accelerated particle abundances; however, all individual accelerated ions were assumed to have the same spectral form. Besides obtaining target and

Table 1. Ambient medium abundances from the full-fit gamma–ray analysis compared with photospheric abundances [from Ramaty *et al.* (*16*)].

Element	Gamma-ray abundances	Photospheric abundances
^{4}He	195 ± 28	269^{+23}_{-21}
C	1.00 ± 0.18	$1.00^{+0.03}_{-0.09}$
N	<0.82	$0.31^{+0.03}_{-0.03}$
O	2.40 ± 0.28	$2.34^{+0.20}_{-0.18}$
Ne	0.86 ± 0.14	$0.34^{+0.09}_{-0.07}$
Mg	0.24 ± 0.11	$0.105^{+0.013}_{-0.011}$
Si	0.47 ± 0.15	$0.098^{+0.012}_{-0.011}$
Fe	0.26 ± 0.11	$0.130^{+0.009}_{-0.009}$

accelerated particle abundances, the best fits for several other parameters could be determined: the power-law exponent, s, for the bremsstrahlung component; the accelerated α particle to proton ratio (α/p); and the spectral parameter (αT) for accelerated particles having a Bessel function spectral form, which results from stochastic acceleration of ions (see below). The target abundances for the best-fit values for αT, s, and α/p = 0.2 are shown in Table 1, and are compared with recent photospheric values in (*16*). The more comprehensive analysis (*13*) gives results similar to the previous ones (*14*), with the elements above oxygen having abundances enhanced over the photospheric values as shown in the table. This basic result from the γ-ray observations is somewhat of a surprise since it suggests that the interaction region is not in the photosphere. However, it has usually been believed (*19*) that the target for the nuclear reactions has been at densities well in excess of 4×10^{11} cm^{-3}. Furthermore, detailed studies (*20*) of the depth distribution of prompt nuclear de-excitation lines show that the maximum of the line production should be at ambient densities exceeding 10^{15} cm^{-3}. One therefore expects that the narrow γ-ray line fluxes which are most sensitive to the target abundances should reflect those in the interaction region. There is also evidence that some SEP events have abundances of elements above oxygen, enhanced over the coronal values. This is also the case for flares that are enriched in ^{3}He (*21*). (See the later discussion on SEP events.)

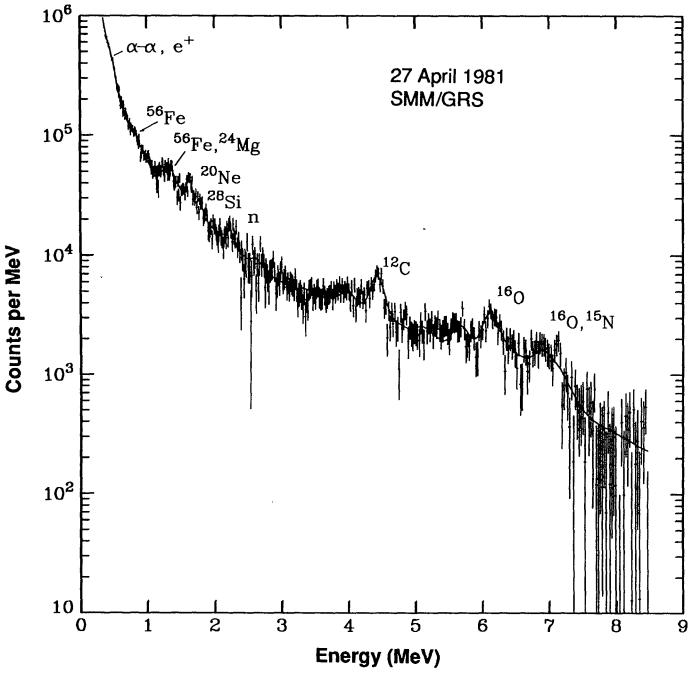

Fig. 1. The γ-ray spectrum observed (*13*) by the SMM GRS for the 27 April 1981 flare. The smooth curve is based on an analysis by Murphy *et al.* (1990) (*18*).

Neutral emissions above 10 MeV. Emission from one of the most intense flares in cycle 21 was recorded by the SMM GRS on 3 June 1982. Figure 2 shows the time history of the count rates in several energy bands extending from 56 keV to over 25 MeV (*22*). A study of data for this event (*23*) indicates that nuclear line emission was present throughout the event, but electron bremsstrahlung above 10 MeV was intense only in the time interval 1142:44 to 1143:49 UT with the spectrum hardening above 40 MeV indicative of a contribution from meson decay γ-rays (*24*). The decay of neutral π^0 mesons (meanlife ~ 10^{-16} s) gives a broad spectrum extending from tens of MeV, to over a hundred MeV with a centroid peak at ~69 MeV and the electrons resulting from the decay of charged mesons [$\pi^{\pm} \rightarrow \mu^+(\mu^-) + \nu_\mu(\bar{\nu}_\mu) \rightarrow e^+(e^-) + \nu_e(\bar{\nu}_e)$] produce a further contribution to the electron bremsstrahlung continuum. The detailed analysis of the spectrum above 10 MeV in this time interval

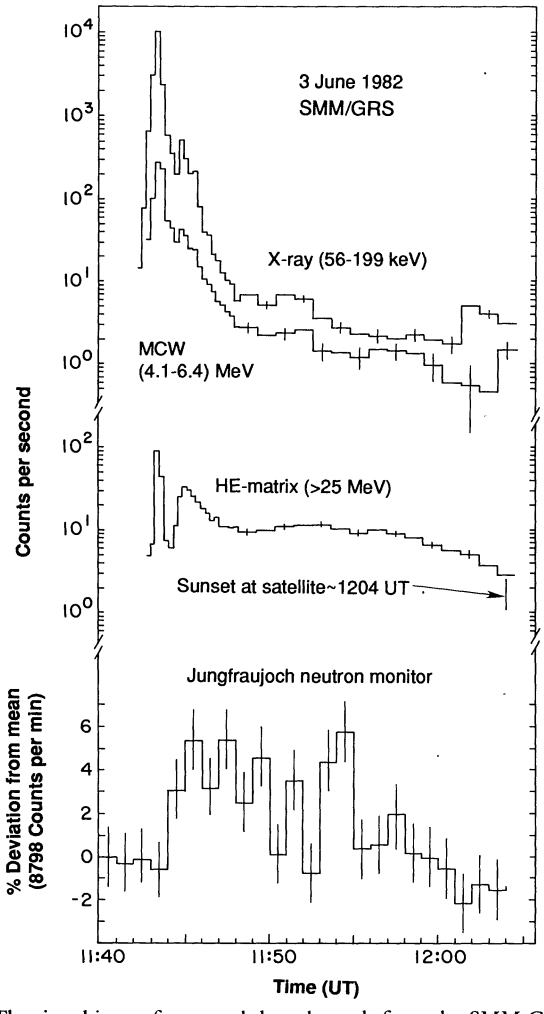

Fig. 2. The time history for several data channels from the SMM GRS and for the Jungfraujoch neutron monitor count rate for the 3 June 1982 flare. Peak count rates in the GRS (x-ray) and main channel window (MCW), 4.1- to 6.4-MeV energy bands are uncertain because of pulse pile-up, excessive dead time, and photomultiplier gain shifts, and should be used with care. The highest MCW count rates have been estimated using measured live time values, averaged over 16.384 s, and a derived gain shift correction. Error bars are 1 σ based on count statistics only [after Chupp *et al.* (*22*)]. [Reprinted courtesy of the authors and the *Astrophysical Journal* published by the University of Chicago Press. ©1986 The American Astronomical Society]

(*24*) shows that it is best explained by three components consisting of a power-law bremsstrahlung spectrum from primary electrons, a π^0 meson decay γ-ray spectrum, and a meson decay electron bremsstrahlung γ-ray spectrum. The π^0 decay γ-rays contribute an integrated flux of ~12 photons cm^{-2} in the initial impulsive time interval (*24*).

After the initial impulsive emission of photons described above, emission continued in all energy bands until satellite sunset. In particular, the large energy-loss events, above 25 MeV, indicated in Fig. 2, do not fall in time as rapidly as the lower energy x-rays. The detailed analysis of this event has shown that this time-extended emission results primarily from meson decay γ-rays (*24*) and higher energy neutrons (*22*) which reach Earth. During the time of secondary, enhanced high-energy emission (see Fig. 2), from 1146:00 UT to 1147:06 UT, there is only evidence for meson decay γ-rays and no primary electron bremsstrahlung component. During the full period of extended emission, from 1146:00 UT until satellite sunset at ~1203 UT, the integrated flux of γ-rays from neutral pion decay is ~45 photons cm^{-2} (*24*). This indicates that >80% of the pion production at the Sun occurred after the initial impulse of the flare, with no clear evidence for high-energy electron production (>10 MeV), as was the case earlier. It has been suggested (*25*) that the high-energy photon emissions observed in this event are evidence for a two-stage (phase) acceleration process, similar to that suggested by the early radio observations (*3*). This view should be considered tentative, since the possibility of coronal storage and later precipitation of the accelerated ions have yet to be thoroughly investigated.

As the extended high-energy emission continues, the SMM GRS energy-loss spectrum shows evidence for a flux of neutrons, which reach Earth, consistent with the enhanced Jungfraujoch neutron monitor count rate (see Fig. 2) which resulted from an atmospheric nucleonic cascade produced by a direct flux of high-energy neutrons from the sun (*26*). With the combined GRS and neutron monitor count rate data and a model of high-energy neutron production, which follows the π^0 meson production time history, allowable neutron production spectra, at the sun, have been determined (*22*). The results, shown in Fig. 3, give the time-integrated, directional solar neutron emissivity spectrum for two acceptable spectral shapes.

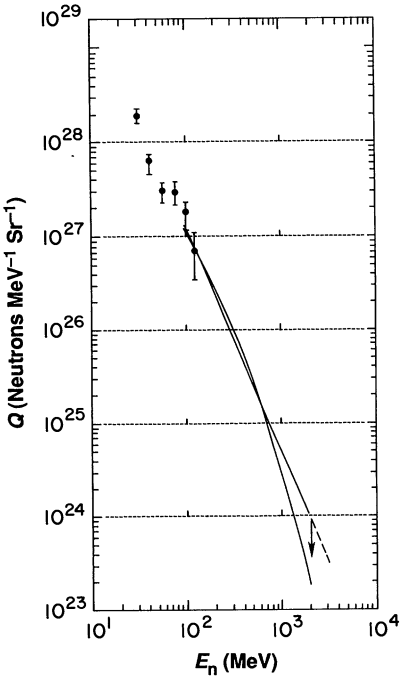

Fig. 3. The time-integrated directional solar neutron emissivity spectrum is shown for flare 2 with best-fit power-law and Bessel-function neutron spectral forms with parameters $s = 2.4$ and $\alpha T = 0.07$, respectively. The data used for the fit are from neutrons arriving, at Earth, over the time period 1144 UT to ~1200 UT. Data points from the neutron decay proton observations (*27*) are also shown [after Chupp *et al.* (*22*)]. Errors bars are 1 σ based on count statistics only. [Reprinted courtesy of the authors and the *Astrophysical Journal* published by the University of Chicago Press. ©1986 The American Astronomical Society]

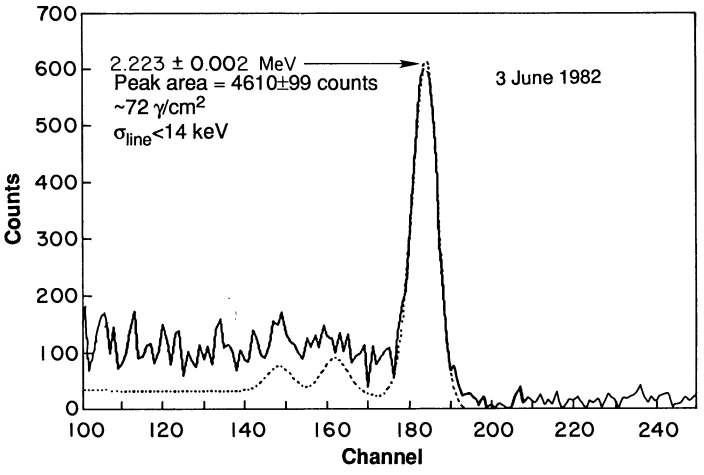

Fig. 4. The SMM GRS γ-ray spectrum near the energy of the neutron-proton capture line during the post-impulsive phase of the 3 June 1982 flare. The solid curve is the total counts observed in each GRS channel over the time period from 11:46:33 UT to 11:52:01 UT. The dotted curve shows the best fit to the line with the measured SMM GRS response function to a Gaussian primary line, single and double escape peaks, and the Compton continuum [after Chupp (*32*)].

One form, a power law in neutron energy with negative exponent 2.4, must be truncated at ~2 GeV, otherwise the neutron monitor would have had a greater initial response than observed. The other spectral form, mathematically a Bessel function of order 2, has a curvature which depletes the GeV neutrons such that no cutoff is needed. The points on the neutron emissivity spectrum shown in Fig. 3, at energies below 100 MeV, are based on the spectrum of the protons, observed in space, which result from inflight decay of neutrons from the sun (*27*). Current use of this technique, with proton detectors on the ISEE-3 (ICE) and Imp spacecrafts, give the neutron flux above about 20 MeV. At lower energies a crude estimate of the spectrum is possible, by means of the capture line at 2.223 MeV. The study (*22*) of high-energy neutrons and the meson decay γ-rays in the 3 June 1982 flare have shown that GeV ions can be accelerated with 100-MeV electrons in a time scale of <16 s.

Neutron capture γ-ray line. This line is the strongest individual line from disk flares; however, because of its photospheric origin it is strongly attenuated in a limb flare (*28*), as was the case for the flare producing the spectrum shown in Fig. 1. In Fig. 4, we show a portion of the SMM GRS spectrum encompassing the 2.223 MeV line for the 3 June 1982 flare which occurred at the heliocentric coordinates S09 E71. The time history of the intensity of this line is shown in Fig. 5 (*29*), and is determined largely by the loss processes which deplete the neutron density in the photosphere. These processes include radiative capture on protons, nonradiative capture in He^3, scattering out of the photosphere, and radioactive decay (*28, 30*). Most of the neutrons, producing this line, were injected during the initial burst in this event; however, neutron-emitting reactions continued at a lower level throughout the event, as indicated by the MCW rates in Fig. 2. Analysis of these data, taking into account the continuous injection of neutrons, gives a best-fit value for the mean loss time of the neutrons as $\tau_{loss} = (89 \pm 10)$ s (*29*). Further analysis of these data give the time-integrated fluence for the line as 314 γ cm^{-2} (*29*) and the $^3He/H$ ratio as $(2.3 \pm 1.2) \times 10^{-5}$ (*30*).

At photon energies below the capture line (see Fig. 4), a low-energy tail appears that indicates excess γ-rays coming from the Sun, above that expected from nuclear de-excitation contributions. A possible cause of this excess is due to Compton photons generated by 2.223 MeV γ-ray scattering in the photosphere. Recent analysis

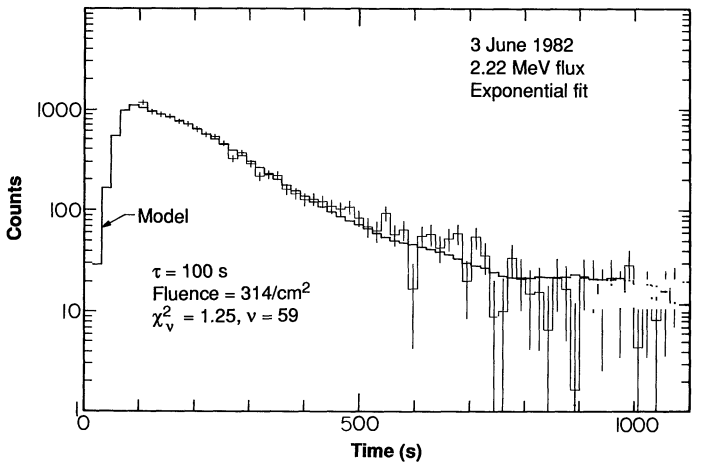

Fig. 5. Time history of the 2.223-MeV γ-ray line flux during the 3 June 1982 flare. The thin-line histogram, with 1 σ error bars, shows the observed counts in the line in 16-s time bins of the SMM GRS. The darker line histogram shows the best fit predicted time history for a single exponential decay with a model of neutron production which is proportional to the observed flux of prompt nuclear γ-rays in the 4.1- to 6.4-MeV GRS energy band [after Prince *et al.* (*29*)].

(*31*) has shown that the ratio of the intensity of the photospheric Compton continuum to the intensity of the neutron capture line can be used to determine the degree of beaming of the primary neutrons into the photosphere.

Temporal characteristics of γ-ray events. A comparison of flare emission time histories at different energies could reveal salient properties of the particle acceleration mechanisms. The SMM GRS γ-ray observations show that the range of event durations runs from ~10 s to over 20 min. Most events include several emission pulses, which can be as short as 10 s or as long as 2 min in an event of ~20-min duration (*17*). The shortest pulses are similar to the reported "elementary flare bursts" (EFBs) in hard x-rays < 100 keV (*32*), with widths varying between 4 ± 1 s and 24 ± 5 s for different flares. At lower photon energies (<270 keV), structure is observed down to ~0.1 s within longer (~2 s) bursts (*33*). In a study of several SMM GRS events (*34*), it was found that the time of the maximum count rate in an individual burst in the 4.1 to 6.4 MeV energy band occurred between 2 s and 45 s later than the corresponding maximum for the hard x-rays >270 keV, with the retardation observed to be proportional to the pulse rise time.

Simultaneous peaking of low-energy (>100 keV) and high-energy (>10 MeV) photons is also observed, limited only by the GRS time resolution. Figure 6 shows the count rates for a flare with several pulses of photons extending from 40 keV to 25 MeV, all occurring within a time interval of 2 min. At ~1249 UT, photons having energies <300 keV were strongly attenuated by the atmosphere, since SMM was just entering sunlight. The peak intensities for the third impulse at ~1250 UT occur simultaneously at all photon energies to within ~±1 s. This means that either the particles producing the energetic photon emission up to >25 MeV were injected into and interacted with the target medium at the same time (≲1 s), or else they were produced (accelerated) in the target medium at the same time (*35*).

Electron-dominated events. During sunspot cycle 21, it was already evident (*36*) that the intensity of the photon emission in the MeV region due to electron bremsstrahlung is highly variable compared to the nuclear line intensity. Thus, in a few intense events nuclear line emission is relatively weak. An outstanding example of this was recently reported (*37*), in a study of the series of intense flares which erupted during March 1989. Figure 7 shows a portion of the time history, for several energy bands, for the 6 March 1989 event, which began at ~1357 UT. During Interval 1 (1357:12 to 1358:50 UT) and Interval 2 (1359:23 to 1359:39 UT), intense emission occurred extending above 40 MeV. Analysis of the energy spectra in these intervals indicates a strong continuum from x-ray energies to 60 MeV, with a rapid falloff above this energy and, most importantly, only weak nuclear line emission. The spectra are uniquely different from the "so-called" γ-ray line events that characterized the majority of the flares seen by the GRS in cycle 22, and one might interpret these observations as indicative of electron acceleration being more efficient than ion acceleration. It should be noted, however, that the photons are secondary radiations, and transport of electrons and ions to the target regions may be a major factor in determining relative photon intensities at a given time. In any case, the most straightforward interpretation of the predominantly continuous spectrum in the two intervals mentioned is bremsstrahlung from a nearly monoenergetic beam of electrons (*37*). About 40 min after initiation of this event, nuclear line emission becomes relatively more intense.

Solar energetic particles (SEPs). The first observed ground-level increases (GLE) in cosmic-ray intensity monitors, associated with solar flares, occurred in 1942 and 1946 (*38*). By using Earth's magnetic field as a momentum analyzer, it has been established that the high-energy protons reaching the Earth have had energies in excess of 20 GeV (*2, 39*). However, the observations cannot precisely determine the time of acceleration of the particles at the Sun, because of uncertainties of their actual trajectories in the interplanetary magnetic fields.

These pioneering observations were followed by others utilizing secondary neutron monitors, balloon-borne charged particle detectors, riometers (relative ionospheric opacity meters), and more recently, particle detectors on spacecraft near Earth (such as IMP

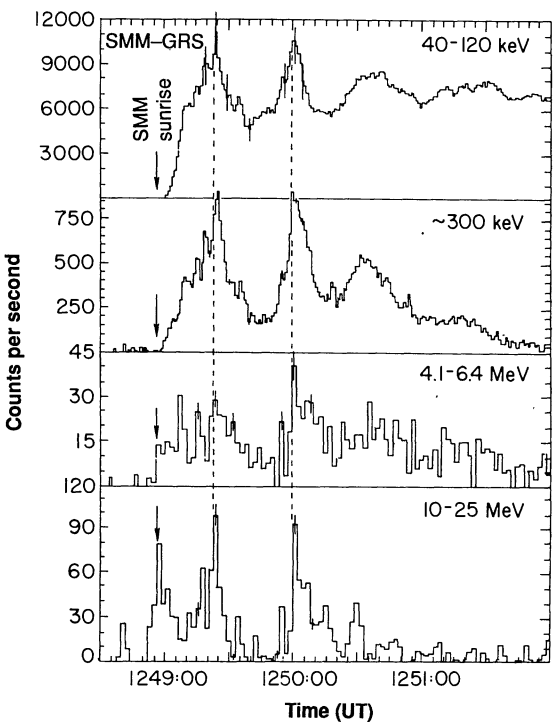

Fig. 6. The time history of photon emissions from 40 keV to ~25 MeV is shown for the flare on 8 February 1982, which occurred before 1249 UT. Early in the flare, low-energy photons <300 keV are occulted by Earth's atmosphere. The times of the peak intensity for the pulse at ~1250 UT are the same to within 2 s for all photon energies. Errors bars are 1 σ based on count statistics only [after Chupp *et al.* (*32*)].

and ISEE-3) and closer to the sun (Helios 1 and 2). The particle detectors on spacecraft typically record the fluxes of ions with energies up to a few hundred MeV per nucleon and electrons with energies to a few tens of MeV. These observations have dramatically increased the data base available, because low-energy ions produced by the Sun (only detectable in space) are observed several times per month, near the sunspot maximum, whereas the relativistic particles, which signal their arrival by an increased count rate in the ground-level cosmic ray monitors, occur infrequently, approximately every 4 years. In cases when a specific particle increase in space can be associated with a particular solar flare, the number of particles emitted by the flare can be estimated by means of an argument from simple diffusion theory. Here it is assumed that the peak intensity of a particle event is a direct measure of the number of particles injected into a magnetic trapping volume—this procedure is called the time of maximum (TOM) method (*40*). If all SEPs were from the same population of accelerated ions which produced the γ-ray emission one would expect a close correlation of the peak SEP intensities with the fluence of nuclear γ rays. Such a correlation has not been found (*7*), which implies that either the TOM technique is not universally valid, or that the γ-ray producing particles and the SEPs come from two different processes.

A comparison (*41*) of electron observations at 1 AU on (ISEE) and on the Helios spacecraft at 0.5 AU suggest that electrons arrive at Helios without scattering, while the electrons which are observed at ISEE have undergone diffusion. In a related study (*42*), five events showed that electron injection occurred simultaneously with particle acceleration as indicated by the initiation of radio bursts. Thus, it is clear that more SEP observations closer to the Sun will be needed to precisely determine the initial flare properties of the SEPs, particularly their time of production. The observations of 200-MeV protons by detectors on Helios (*40*) have also shown a striking correlation with the γ-ray observations for the 3 June 1982 event. Because of the fortuitous location of Helios and the flare on the east side of the Sun, SEP propagation to the Helios spacecraft was very direct, and there is a strong indication that both the SEP and the γ-ray producing protons were accelerated at the same time (*40*)!

Available SEP data suggest that there may be (at least) two processes responsible for their production at the Sun. When the SEP events were divided into two classes, according to their soft x-ray duration (*43*) (impulsive or gradual), it was found (*44*) that the average electron/proton ratio was considerably larger (>10) for those in the "impulsive class" than for those in the "gradual class." Also, the time scales of the SEP events in the "impulsive class" were shorter than for those in the "gradual class." It was also found (*45*) that the electron rigidity spectra for SEPs divide into two classes consistent with the impulsive and gradual classifications just mentioned (*44*). The electron events corresponding to the impulsive class had spectra that are harder at high rigidities (>1 MV) and also have γ-ray line emission (*46*). Electron events which fit the impulsive class and were observed between 1980 and 1982 all had higher $^3He/^4He$ values and were SMM GRS flares (*47*).

It is of particular interest that events in the impulsive class have enhanced abundances of $^3He/^4H$ and sometimes heavy elements such as Fe/O (*16, 21*) over the "normal" coronal abundances. These correlations are not always seen on an event-by-event basis, however, and it seems possible that the temperature in the acceleration region which controls the degree of ionization of the ions, and hence their gyrofrequency, may be responsible for the lack of a perfect correlation (*21*).

Acceleration Mechanisms

Our knowledge of the characteristics of the particles accelerated in flares has increased dramatically in the past 10 years, but further refinements are needed in order to locate the regions where particle acceleration and interactions occur. It is expected that in the future, high–spatial resolution observations by the Orbiting Solar Laboratory (OSL) at optical to soft x-ray wavelengths and corresponding high–energy resolution observations of the energetic neutral γ-ray and neutron emissions will make a qualitative advance in resolving the flare problem. Until we have this vital new information, we must be content to investigate the applicability of all the known acceleration processes.

These may be categorized as follows: (i) First-order Fermi or diffusive shock acceleration, (ii) second-order Fermi or diffusion in momentum space, and (iii) coherent processes involving electric fields generated by a variety of plasma processes. Before discussing these mechanisms, it must be realized that the acceleration must take place in a geometry containing strong (100 to 1000 G) magnetic fields in open or closed configurations and that the transport of

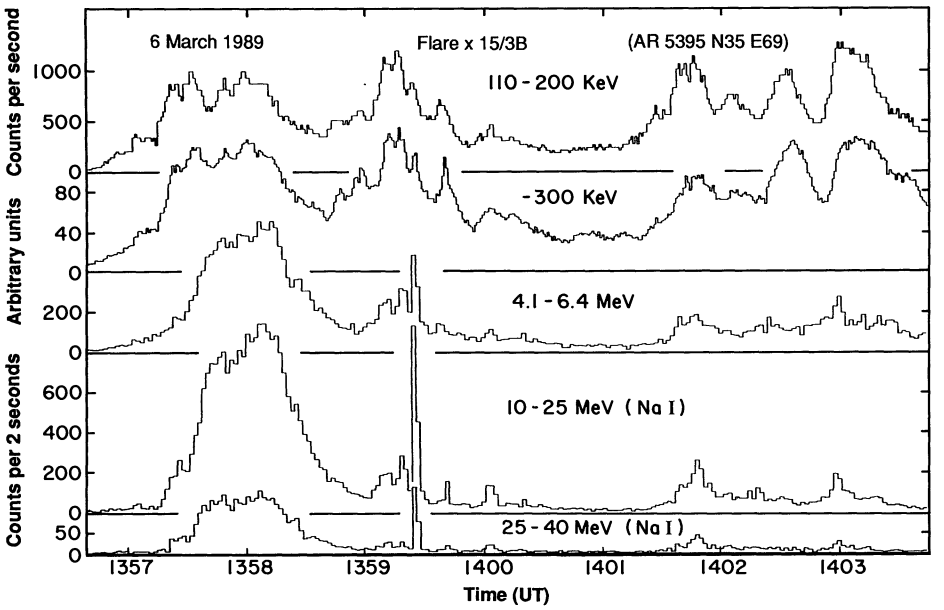

Fig. 7. A partial time history of photon emissions in several energy channels for the cycle 22 flare on 6 March 1989 which was initiated in hard x-rays at ~1357 UT. In the time intervals 1357:12 to 1358:50 UT and 1359:23 to 1359:39 UT the photon spectra are dominated by primary electron bremsstrahlung. The total duration of the event seen by the SMM GRS was over 1 hour. [Figure courtesy of E. Rieger and H. Marschhäuser, Max Planck Institute of Extraterrestrial Physics (*37*)]

particles during and after acceleration plays a vital role. For example, the gyroradius of a 10-MeV electron in a 500-Gauss field is ~0.7 m and for a GeV proton it is ~57 m, so the particle trajectories follow closely the magnetic field topology. In either case, this size scale is far below that discernable with the best optical telescopes (1 arc sec ~750 km), and there may be transient structures in the magnetic field of such small scale size. The importance of the geometry can also be appreciated by considering the escape time of an ion from a flare loop due to curvature drift which, for typical loop conditions, can be estimated (*48*) as >2 hours for a 10-MeV electron and >2 min for a 1-GeV proton, depending on the pitch angle of the particles.

I do not intend to give an exhaustive review of the vast literature in solar flare particle acceleration but rather to describe, briefly, those mechanisms that seem to show the most applicability to the current problem. Any attempt to determine which acceleration mechanisms will explain the observational data must consider the following facts:

1) Ion and electron acceleration is observed frequently in flares (*17*), but the electron-to-ion ratio is highly variable.

2) Relativistic electrons (100 MeV) and ions (GeV) can be accelerated together in time scales <16 s (*22*).

3) In at least one intense γ-ray event, ions of GeV energy were apparently continually produced or released from storage for greater than 20 min, but without corresponding precipitation of relativistic electrons ($\gamma > 20$) (*24*).

4) The interaction region for accelerated ions producing γ-rays is more characteristic of normal coronal rather than photospheric abundances (*16*) and must have a density $n \gtrsim 10^{12}$ cm^{-3} (*19*).

5) Electron-dominated events can occur due to transient acceleration of electrons with energies >10 MeV in <2 s (*37*).

6) There is an apparent poor correlation of the number of ions which produce γ-rays with the number of SEPs released into the interplanetary medium (*7*).

7) Strong evidence exists for two classes of SEP events. One class includes events which are impulsive in time, have γ-ray line emission, larger-than-normal ^{3}He/^{4}He, e/p, and α/p ratios, are usually rich in MeV electrons, and have enhanced heavy-nuclide abundances ($Z > 8$). The second class of events has abundances very similar to those of the ambient corona (*16, 21*).

Shock drift and first-order Fermi acceleration. Solar flare particle acceleration by shocks has been extensively studied (*49*). If a fast-mode magnetohydrodynamic (MHD) shock $v_s >> c_s$ is formed during or after the initial flare energy release, acceleration can take place by one of two means. Here v_s and c_s are the shock velocity and sound velocity, respectively.

In one case, if no wave activity exists upstream or downstream of the shock (a highly idealized situation), then a particle with initial energy E_0 can be trapped in the shock and be accelerated as it drifts along the induced convection field $\mathbf{E} = -\mathbf{v}_s \times \mathbf{B}$, where $\mathbf{B}$ is the magnetic field. This "shock drift" mechanism can give a rapid energy gain to only a few times the injection energy E_0 for quasiperpendicular shocks, where the local magnetic field is more or less perpendicular to the shock velocity vector (*50*). A detailed analysis (*51*) indicates that nonrelativistic particles can achieve an energy of $13 \times E_0$ and ultra relativistic particles an energy $7E_0$.

The second, more promising, case of shock acceleration arises if there is upstream and downstream turbulence, so that the particles crossing the shock can scatter back and forth, be trapped in the shock, and are accelerated in each cycle as they cross the front. The fractional energy gain in this process is $\propto v_s/c$ and is therefore called first-order Fermi or diffusive shock acceleration. This mechanism is well developed theoretically since shock-accelerated particles are commonly observed, in situ, in interplanetary solar flare shocks and planetary bow shocks (*1, 50, 52*). The acceleration time for ions in a flare-generated quasi-parallel shock can be very fast (~1 s) (*49*), if it is assumed that the ions are injected into a preexisting shock. Acceleration of electrons, however, requires very high injection energies (~100 keV) (*49*), so this mechanism alone cannot explain all the flare emissions. The diffusive shock acceleration mechanism is very attractive; however, in order to explain the neutral flare emissions the shock must be fully developed and efficiently accelerate ions at the flare energy release site (*53*), in subsecond time scales, which is necessary to explain much of the neutral flare emission.

Second-order Fermi or stochastic acceleration. In the classic Fermi process (*54*), where ions collide with randomly moving magnetic clouds, the fractional energy gain per collision is proportional to the average square of the velocity, δv^2, of the clouds (*55*), hence the connotation "second-order" Fermi. Detailed general treatments (*55*) describe the acceleration as diffusion in momentum space. This model has received considerable attention in the solar flare case since it can be expected that a turbulent medium must surely be present in the aftermath of a flare. Solution of a Fokker-Planck equation in momentum space, assuming an energy-independent (constant) mean free path, λ, between scatterings, and containment time T (*56*), give a two-parameter solution for the accelerated ion energy spectrum that fits many of the SEP spectra observed in space. The two parameters are the acceleration efficiency $\alpha = (\delta v^2/\lambda c)$ and the containment time T. These may be adjusted to give ion spectra which can explain the observed γ-ray and neutron spectra.

Further refinements (*57*) have postulated for ion acceleration, gyroresonant scattering with a Kolmogorov spectrum of stochastic MHD waves. In this model the flare is assumed to occur (with the desired spectrum of turbulence) in a magnetic loop whose ends are tied to the photosphere, and the Fokker-Planck equation is solved numerically for the time-dependent accelerated ion spectrum. Accelerated particles whose pitch-angles end up in the loss cone will precipitate into the photosphere, giving a time-dependent burst of neutral radiation. The acceleration of electrons is accomplished by resonant scattering with whistler waves (*57*). Such a model can conceivably explain the rise time of short impulsive γ-ray bursts if the turbulence is assumed to have the right time dependence. The decline of the γ-ray burst in this case must be controlled by transport of the precipitating ions and electrons (*58*). The essential condition that must be satisfied for stochastic mechanisms to be applicable for fast solar flares is the rapid development of a physically plausible spectrum of turbulence. The dependence of the acceleration efficiency, α, on the turbulence spectrum and particle energy has been recently considered (*59*). However, the physical basis of an energy-independent containment time, T, used in the work to date has not been discussed.

Direct electric field and other coherent mechanisms. One of the earliest mechanisms proposed for the acceleration of flare particles is a transient electric field which would accelerate electrons and ions in opposite directions (*60*). Indeed, the existence of impulsive bursts of electron-dominated events, described above (*37*), suggests that a nearly monoenergetic beam of electrons directed into the solar atmosphere could explain the hard γ-ray bursts shown in Fig. 7. These observations imply that a transient electric field E, of scale length d, provides a potential drop $d \cdot E \sim 100$ MV, which must be maintained for time periods ranging from a few seconds to 30 s.

A recent review (*61*) of solar flare particle acceleration classifies all mechanisms which involve generation of an electric field as coherent processes. For example, electric fields can be produced in a current sheet, perpendicular to the magnetic field, giving an electric field $\mathbf{E}_0 = nJ_0\hat{\mathbf{e}}_z$ (*61*). Also an electric field $\mathbf{E} = -\mathbf{v} \times \mathbf{B}$ can be induced as a result of the flow velocity $\mathbf{v}$ of material outside the current sheet. Numerous schemes to accelerate particles during magnetic recon-

nection have been studied in detail and discussed in several reviews [see (*50, 61, 62*)]. The possibility of particle acceleration when the electric field or currents are parallel to the magnetic field have also been considered (*63*). It is noteworthy that magnetic reconnection in the Earth's magnetopause does actually occur (*64*) and during the magnetic substorm, ions (and electrons) are impulsively accelerated, to energies of 1 MeV or more (*65*). The similarity of auroral particle acceleration to the solar flare case has suggested to several authors (*66, 67*) that the same acceleration mechanisms may explain both phenomena. An application of reconnection theory in a specific loop coalescence model of solar flares has been compared to the γ-ray observations in several solar flares (*68*) with generally good agreement.

Short spikes (<100 ms) of decimetric radio emission are sometimes seen in association with groups of metric Type III radio bursts and are closely associated in time with (>30 keV) hard x-ray bursts (*62*). The radio spikes are narrow band (3 to 10) MHz, at 500 MHz and have an estimated source size of <100 km, with a brightness temperature of $\sim 10^{15}$ K implying a coherent radiation mechanism (*62*). The possibility that these narrow band electromagnetic waves could also accelerate electrons in the ambient plasma has been investigated recently (*69*) and may be an effective way of transferring energy from inside closed loops to external plasma electrons.

Conclusions

It is gratifying that there have been considerable advances in the experimental and theoretical understanding of the various possible mechanisms that can accelerate solar flares. It is hoped that in the future more refined high-resolution observations will be made of solar active regions in the optical and soft x-ray energy bands. Coordinated vector magnetic field measurements during flares and improved observations of the energetic solar neutral emissions with high-energy and spatial resolution will provide knowledge of the parameters needed by theory to evaluate specific flare models. It seems likely that more than one acceleration mechanism may be necessary to explain all observations.

REFERENCES AND NOTES

1. J. A. Simpson, *Adv. Space Res.* **9**, 5 (1989).
2. D. B. Swinson and M. A. Shea, *Geophys. Rev. Lett.*, **17**, 1073 (1990).
3. J. P. Wild, *Phys. Soc. Jpn.* **17**, 249 (1962); J. P. Wild, S. F. Smerd, A. A. Weiss, *Annu. Rev. Astron. Astrophys.* **1**, 291 (1963); J. P. Wild and S. F. Smerd, *ibid.* **10**, 159 (1972).
4. E. L. Chupp *et al.*, *Nature* **241**, 333 (1973); E. L. Chupp, D. J. Forrest, A. N. Suri, in *Solar Gamma X- and EUV-Radiation, IAU Symp. 68*, S. R. Kane, Ed. (Reidel, Dordrecht, 1975), p. 341.
5. D. J. Forrest and E. L. Chupp, *Nature* **305**, 291 (1983).
6. M. Yoshimori *et al.*, *Proc. XVIII Int. Cosm. Ray Conf.* **4**, 89 (1983); M. Yoshimori, *Space Sci. Rev.* **51**, 85 (1989).
7. E. Cliver *et al.*, *Proc. XX Int. Cosm. Ray Conf.* **3**, 61 (1987).
8. R. E. Lingenfelter and R. Ramaty, in *High Energy Nuclear Reactions in Astrophysics*, B. S. P. Shen, Ed. (Benjamin, New York, 1967), p. 99.
9. P. Morrison, *Nuovo Cimento* 7, 858 (1958).
10. B. R. Dennis and R. A. Schwartz, *Sol. Phys.* **121**, 75 (1989).
11. H. S. Hudson *et al.*, *Astrophys. J.* **236**, L91 (1980); T. A. Prince, J. C. Ling, W. A. Mahoney, G. R. Riegler, A. S. Jacobson, *ibid.* **255**, L81 (1982).
12. D. J. Forrest *et al.*, *Sol. Phys.* **65**, 15 (1980).
13. R. J. Murphy, G. H. Share, J. R. Letaw, D. J. Forrest, *Astrophys. J.* **358**, 298 (1990).
14. R. J. Murphy, R. Ramaty, D. J. Forrest, B. Kozlovsky, *Proc. XIX Int. Cosm. Ray Conf.* **4**, 249, 253 (1985).
15. R. Ramaty, R. J. Murphy, B. Kozlovsky, R. E. Lingenfelter, *Sol. Phys.* **86**, 395 (1983).
16. R. Ramaty, R. J. Murphy, J. A. Miller, in *Particle Astrophysics*, V. Jones, F. Kerr, J. Ormes, Eds. (American Institute of Physics, New York, 1990), p. 143.
17. D. J. Forrest, in *Positron-Electron Pairs in Astrophysics*, M. L. Burns, A. K. Harding, R. Ramaty, Eds. (American Institute of Physics, New York, 1983), p. 3.
18. R. Murphy, R. Ramaty, B. Kozlovsky, D. V. Reames, in preparation.
19. R. Ramaty and R. J. Murphy, *Space Sci. Rev.* **45**, 213 (1987).
20. X.-M. Hua, R. Ramaty, R. E. Lingenfelter, *Astrophys. J.* **341**, 516 (1989).
21. D. V. Reames, *Astrophys. J. Suppl.* **73**, 235 (1990).
22. E. L. Chupp *et al.*, *Astrophys. J.* **318**, 913 (1987).
23. E. L. Chupp, *Astrophys. J. Suppl.* **73**, 213 (1990).
24. D. J. Forrest *et al.*, *Proc. XIX Int. Cosm. Ray Conf.* **4**, 146 (1985).
25. R. J. Murphy, C. Dermer, R. Ramaty, *Astrophys. J. Suppl.* **33**, 721 (1987).
26. H. Debrunner, E. Flückiger, E. L. Chupp, D. J. Forrest, *Proc. XVIII Int. Cosm. Ray Conf.* **4**, 75 (1983).
27. P. Evenson, P. Meyer, K. R. Pyle, *Astrophys. J.* **274**, 875 (1983).
28. H. T. Wang and R. Ramaty, *Sol. Phys.* **36**, 129 (1974).
29. T. A. Prince, D. J. Forrest, E. L. Chupp, G. Kanbach, G. H. Share, *Proc. XVIII Int. Cosm. Ray Conf.* **4**, 79 (1983).
30. X-M. Hua and R. E. Lingenfelter, *Astrophys. J.* **319**, 555 (1987).
31. W. T. Vestrand, *ibid.* **352**, 353 (1990).
32. See E. L. Chupp, *Phys. Scr.* **T18**, 5 (1987) and references therein.
33. A. L. Kiplinger, B. R. Dennis, A. G. Emilie, K. J. Frost, L. E. Orwig, *Sol. Phys.* **86**, 239 (1983).
34. B. M. Gardner *et al.*, *Bull. Am. Astron. Soc.* **13**(4), 903 (1983).
35. S. R. Kane, E. L. Chupp, D. J. Forrest, G. H. Share, E. Rieger, *Astrophys. J. Lett.* **300**, L95 (1986).
36. B. R. Dennis, *Sol. Phys.* **118**, 49 (1988).
37. E. Rieger and H. Marschhäuser, *Proceedings of MAX 91 Workshop #3, Developments in Observation and Theory for Solar Cycle 22*, R. M. Winglee and A. L. Kiplinger, Eds., in preparation.
38. I. Lange and S. E. Forbush, *Terr. Magn. Atmos. Electr.* **47**, 185 (1942); S. E. Forbush, *Phys. Rev.* **70**, 771 (1946); A. Ehmert, *Z. Naturforsch.* **3A**, 264 (1948).
39. P. Meyer, E. N. Parker, J. A. Simpson, *Phys. Rev.* **104**, 768 (1956).
40. M. A. I. Van Hollebeke, F. B. MacDonald, J. P. Meyer, *Astrophys. J. Suppl.* **73**, 285 (1990).
41. W. Dröge, G. Wibberenz, B. Klecker, *Proc. XXI Int. Cosm. Ray Conf.* **5**, 187 (1990).
42. M. B. Kallenrode and G. Wibberenz, *ibid.*, p. 112.
43. R. Pallavicini, S. Serio, G. S. Vaiana, *Astrophys. J.* **216**, 108 (1977).
44. H. V. Cane, R. E. McGuire, T. T. Von Rosenvinge, *ibid.* **301**, 448 (1986).
45. P. Evenson, D. Hovestadt, P. Meyer, D. Moses, *Proc. XIX Int. Cosm. Ray Conf.* **4**, 74 (1985).
46. P. Evenson, P. Meyer, S. Yanagita, D. J. Forrest, *Astrophys. J.* **283**, 439 (1984).
47. P. Evenson, C. Kato, I. Kondo, P. Meyer, S. Yanagita, *Proc. XXI Int. Cosm. Ray Conf.* **5**, 374 (1990).
48. R. Ramaty, J. A. Miller, X-M. Hua, R. E. Lingenfelter, in *Nuclear Spectroscopy of Astrophysical Sources*, N. Gehrels and G. Share, Eds. (American Institute of Physics, New York, 1988), p. 217.
49. D. C. Ellison and R. Ramaty, *Astrophys. J.* **298**, 400 (1985); L. Vlahos *et al.*, *NASA Report C.P. 2439* (NASA, Greenbelt, MD, 1986), chap. 2; R. B. Decker and L. Vlahos, *Astrophys. J.* **306**, 710 (1986).
50. M. Scholer, in *Acceleration of Energetic Particles in Solar Flares in Cool Star Envelopes*, O. Havnes *et al.*, Eds. (Kluwer, Dordrecht, 1988), p. 195.
51. I. N. Toptyghin, *Space Sci. Rev.* **26**, 157 (1980).
52. T. Terasawa and M. Scholer, *Science* **244**, 1050 (1989).
53. M. A. Lee and J. M. Ryan, *Astrophys. J.* **303**, 829 (1986).
54. E. Fermi, *Phys. Rev.* **46**, 973 (1949).
55. R. D. Blanford, in *Magnetospheric Phenomena in Astrophysics*, R. I. Epstein and W. C. Feldman, Eds. (American Institute of Physics, New York, 1986), p. 1.
56. R. Ramaty, in *Particle Acceleration Mechanisms in Astrophysics*, J. Arons, C. McKee, C. Max, Eds. (American Institute of Physics, New York, 1979), p. 135.
57. J. A. Miller, R. Ramaty, N. Guessoum, *Proc. XXI Int. Cosm. Ray Conf.* **5**, 36 (1990).
58. R. Ramaty, J. A. Miller, X-M. Hua, R. E. Lingenfelter, *Astrophys. J. Suppl.* **73**, 199 (1990).
59. J. A. Miller, N. Guessoum, R. Ramaty, *Astrophys. J.* **361**, 701 (1990).
60. R. Giovanelli, *Mon. Not. R. Astron. Soc.* **107**, 338 (1947); S. I. Syrovatskii, in *Solar Flares and Space Research*, C. DeJager and Z. Svestka, Eds. (North-Holland, Amsterdam, 1969), p. 346.
61. L. Vlahos, *Sol. Phys.* **121**, 431 (1989).
62. A. O. Benz, *ibid.* **111**, 1 (1987).
63. S. A. Colgate, *Astrophys. J.* **221**, 1068 (1978); D. S. Spicer, *Space Sci. Rev.* **31**, 351 (1987).
64. G. Paschmann, in *Magnetic Reconnection in Space and Laboratory Plasmas*, E. W. Hones, Jr., Ed. (American Geophysical Union, Washington, DC, 1984), p. 114.
65. R. J. Pellinen and W. J. Heikkila, *J. Geophys. Res.* **83**, 1544 (1978).
66. S.-I. Akasofu, *Sol. Phys.* **64**, 333 (1979).
67. G. Haerendel, *Proceedings of the Joint Varenna-Abastumani Int. School and Workshop on Plasma Astrophysics (ESA SP-285)* **1**, 37 (1988).
68. J. Sakai and Y. Ohsawa, *Space Sci. Rev.* **46**, 113 (1987).
69. P. Sprangle and L. Vlahos, *Astrophys. J.* **273**, L95 (1983).

70. The author gratefully acknowledges critical comments and suggestions on a draft of this paper by R. Ramaty, E. Rieger, and anonymous referees. The author also appreciates the prepublication use of Fig. 1, provided by R. J. Murphy, and Fig. 7, by E. Rieger and H. Marschhäuser. Valuable assistance in the preparation and editing of this manuscript by M. M. Chupp is much appreciated. Support for this work has been provided by the University of New Hampshire, the Max Planck Institute for Extraterrestrial Physics (Garching, FRG), and NASA grant NAG5-720.